

PHOTOLUMINESCENCE AND ELECTRON PARAMAGNETIC RESONANCE OF NITROGEN-DOPED ZINC SELENIDE EPILAYERS

M. MOLDOVAN, S.D. SETZLER, Z. YU, T.H. MYERS, L.E. HALLIBURTON, N.C. GILES
Department of Physics, West Virginia University, Morgantown, WV 26506-6315

ABSTRACT

Photoluminescence (PL) and electron paramagnetic resonance (EPR) studies were performed on a series of ZnSe samples grown by molecular beam epitaxy. The PL has been studied as a function of excitation wavelength, power, temperature, and time. The PL data indicates that the broad emission from a heavily nitrogen-doped ZnSe film is composed of three distinct recombination processes. The EPR spectra taken at 8 K and 9.45 GHz show an isotropic signal at $g = 2.0027(3)$ which we attribute to singly ionized selenium vacancies (V_{Se}^+). The PL and EPR data help to clarify the role of defects in the compensation of heavily nitrogen-doped ZnSe thin films.

INTRODUCTION

In recent years, considerable effort has focused on developing zinc selenide for blue and blue-green lasers and LEDs. Achieving high p-type conductivity continues to be a problem in this material. Nitrogen is a promising dopant for p-type ZnSe, but unwanted compensating centers¹ have limited the maximum achievable carrier density to the low 10^{18} cm^{-3} level. Electron paramagnetic resonance (EPR),² optically detected magnetic resonance (ODMR),^{3,4} and positron annihilation⁵ techniques are being used to establish the identities of these device-limiting centers. Photoluminescence (PL) complements these efforts by providing information about the recombination processes involving the compensating centers.

The PL from ZnSe epilayers grown by molecular beam epitaxy (MBE) changes dramatically as the level of nitrogen doping increases. Heavy nitrogen doping ($> \text{mid-}10^{18} \text{ cm}^{-3}$) is accompanied by a broad luminescence in the region from 2.45 to 2.68 eV. Early explanations⁶⁻⁸ of this deep luminescence have invoked a distribution of spatially separated potential wells due to a local variation in the distribution of charged impurities. A broad band of states leading to DAP recombination involving the isolated nitrogen acceptor and a donor was suggested.

We have performed a PL study of heavily doped ZnSe:N epilayers grown by MBE. Our data suggest that the deep PL emission is more complicated than previously thought. The PL dependence on excitation wavelength, excitation power density, and temperature have been monitored. The time decay of the PL also has been measured. These data distinguish the separate recombination channels involved in the deep-level luminescence. We find that the deep PL consists of three distinct radiative recombination processes. In addition, one of the bands is accompanied by phonon replicas of energy $69 \pm 3 \text{ meV}$. We also have performed EPR studies on a series of ZnSe samples. A signal near $g=2$ is observed in almost all the samples and is assigned to a singly ionized selenium vacancy (V_{Se}^+) center. Its presence correlates with an increase in the Zn-to-Se ratio in the undoped material and with an increase in nitrogen in the doped material. Our observation of large concentrations of single ionized selenium vacancies in ZnSe epilayers provides experimental verification that these native defects may play a significant role in this material.

EXPERIMENT

A series of ZnSe epilayers were grown at West Virginia University in a custom MBE system. These films were grown at 300°C on semi-insulating (100) GaAs substrates using high purity (7N) elemental Zn and Se from conventional MBE sources.⁹ An atomic nitrogen flux from an rf plasma source (Oxford model CARS25) was used for nitrogen doping.

The PL data were obtained under both cw and pulsed excitation conditions. The 325-nm output from a HeCd laser (Liconix model 4240) was focused onto the sample surface for above-band-gap cw excitation. Below-band-gap excitation (458 nm) was provided by an argon ion laser (Coherent Innova 400-10). Time-resolved PL studies were conducted using the 355-nm output from a Q-switched Nd:YAG laser (Continuum model Powerlite 8000-10) operating at 10-Hz repetition rate. The average power incident on the sample was $128 \mu\text{W}/\text{cm}^2$, corresponding to $12.8 \mu\text{J}/\text{cm}^2$ per pulse. The PL produced by pulsed excitation was measured using a digital oscilloscope (Tektronix TDS 684A). The system time-decay response, determined by monitoring the laser pulse, was about 3.5 ns. All PL spectra have been corrected for the response of the detection system.

For the EPR study, a Bruker ESP-300 spectrometer, operating at a microwave frequency of 9.45 GHz, a static-field modulation frequency of 100 kHz, and a microwave power of 5 mW, was used. Glassware from an Oxford Instruments ESR-900 helium gas flow system extended through a standard rectangular TE₁₀₂ microwave cavity and maintained the sample temperature near 8 K during the measurements. The microwave frequency was measured with a Hewlett Packard 5340A counter and the magnetic field was measured with a Varian E-500 digital gaussmeter. A small MgO:Cr crystal was used to correct for the difference in magnetic field between the sample and gaussmeter probe (the isotropic g value for Cr³⁺ in MgO is 1.9800).

RESULTS

Figure 1 shows the PL spectra obtained from a ZnSe epilayer doped with nitrogen ($1.5 \times 10^{19} \text{ cm}^{-3}$ as determined by SIMS). The data were taken at 4.8 K with 325-nm (curve a) and 458-nm (curve b) excitation, and at 90 K with 458-nm excitation (curve c). The incident power density was $2 \text{ W}/\text{cm}^2$. The change in appearance of the luminescence for above- and below-band-gap excitation (compare curves a and b) suggests that two PL bands are present. These bands are labeled N_I and N_{II} . Phonon replicas, spaced by approximately 70 meV, are associated with N_I and are easily seen at higher temperature (curve c). This defect-associated phonon has an energy considerably larger than the 32-meV LO phonon of the ZnSe lattice.

The power dependence of the N_I and N_{II} bands is shown in Fig. 2. These spectra were obtained using above-band-gap excitation (325 nm) and the incident power density was varied by more than three orders of magnitude. The spectra are displaced vertically and are enhanced by the

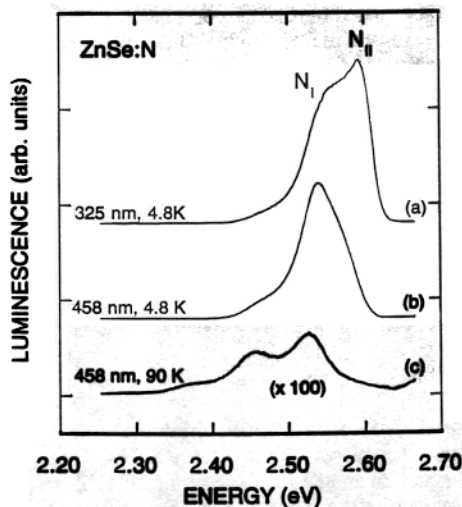


Fig. 1. PL from a heavily nitrogen-doped ZnSe epilayer (a) at 4.8 K using 325-nm excitation, (b) at 4.8 K using 458-nm excitation, and (c) at 90 K using 458-nm excitation.

factors shown on the plots. At the lowest power density shown here (1.4 mW/cm^2), the emission peak corresponding to N_I occurs at about 2.54 eV . As the power density is increased, the peak N_{II} emerges on the high energy side of the spectrum. At the highest power density (5 W/cm^2), the N_{II} band is dominant. The N_{II} band does shift slightly with changes in excitation power.

To determine the peak positions and relative amplitudes of the N_I and N_{II} bands at each incident power density, we performed a least-squares, sum-of-gaussians curve-fitting analysis of the data. As a representative example, the inset to Fig. 2 shows that the PL corresponding to the higher power densities can be described as the sum of three bands. The data from curve c are the dots in the inset, and the superposition of the three bands is the solid line. A similar power dependence study was performed using 458-nm excitation. Based on a curve-fitting analysis of all the power dependence data, the N_I peak does not shift (within our experimental error) as a function of incident excitation power and the N_{II} peak does shift from about 2.55 eV (at low power) to nearly 2.61 eV (at the highest cw powers used in our study). The phonon replica associated with N_I (the lower energy band in the inset to Fig. 2) was found to be $69 \pm 3 \text{ meV}$.

Figure 3 shows the time dependence of the PL emission from the heavily nitrogen-doped ZnSe epilayer. The decay of the PL was sequentially monitored at a series of energies extending from 2.75 eV (4500 \AA) to 2.40 eV (5165 \AA) while pumping with 355-nm light. We then constructed the time evolution of the PL spectrum, by extracting the PL intensity at seven selected times, and the results are shown in Fig. 3(a) on a linear scale and in Fig. 3(b) on a logarithmic scale.

The top curves in Figs. 3(a) and 3(b) show the PL spectrum obtained immediately after the laser pulse. In addition to the N_I and N_{II} bands, the pulsed excitation has produced a third emission band at 2.65 eV which decays quickly. This third band is labeled N_{III} . The time evolution of N_I and N_{II} in Fig. 3 is of interest. Initially, the peak of N_{II} occurs at about 2.61 eV but shifts to lower energy with increasing time. In contrast, the peak position of the N_I band does not shift measurably with time. This difference in behavior for N_I and N_{II} clearly establishes the separate nature of the two recombination paths.

The N_{II} band displays the following characteristics which are consistent¹⁰ with DAP recombination: (i) peak shift to higher energies with increasing excitation power and (ii) peak shift to lower energies with increasing time after pulsed excitation. The lifetime of the N_{III} band is 3.5 ns or less. This short-lifetime behavior is consistent with conduction band to valence band recombination, excitonic recombination, or band-to-impurity recombination. Excitonic recombination is unlikely at this high doping level. A likely possibility for the origin of N_{III} is electron-acceptor

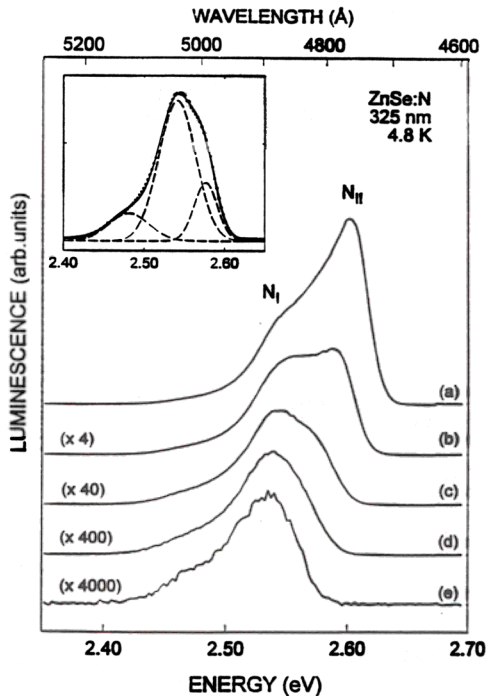


Fig. 2. PL from a heavily nitrogen-doped ZnSe epilayer using 325-nm excitation with incident power densities of (a) 5 W/cm^2 , (b) 1 W/cm^2 , (c) 0.1 mW/cm^2 , (d) 10 mW/cm^2 , and (e) 1.40 mW/cm^2 . The inset shows that the PL from curve c can be described as the sum of three bands.

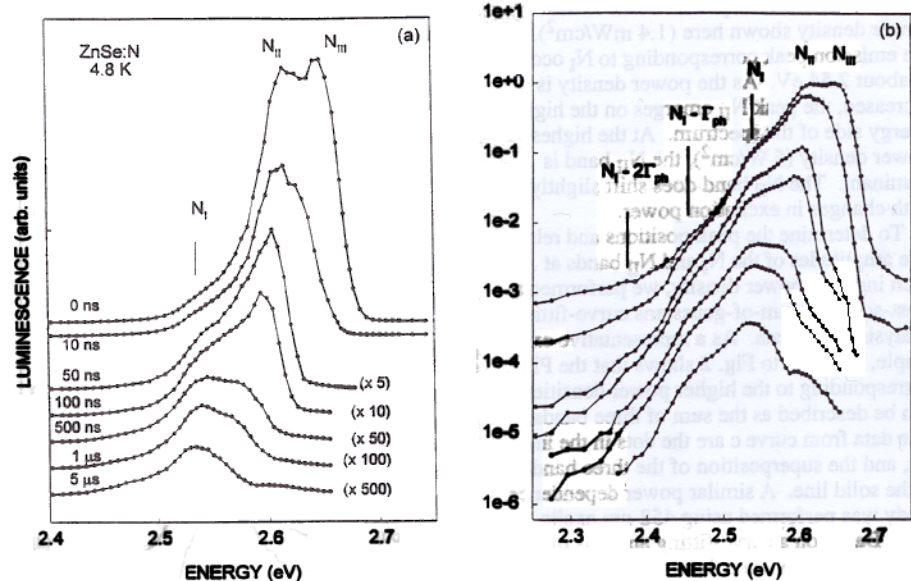


Fig. 3. Time-resolved PL from a ZnSe:N epilayer. (a) Intensities are plotted on a linear scale. Curves are displaced vertically for clarity. Several of the curves have been enhanced by the factors shown. (b) The same spectra are shown on a logarithmic scale.

(e,A) recombination since this band occurs 50 meV above N_{II} , which is DAP recombination. This 50-meV energy agrees closely with the range of values (44 to 57 meV) previously associated with a deep donor in ZnSe:N.¹¹⁻¹⁴ The N_I band shows no shift in peak position with increasing excitation power, no shift in peak position with time, and is accompanied by phonon replicas with energy of about 69 ± 3 meV. The relative intensities of the N_I phonon replicas exhibit a strong temperature dependence. Evidence for the origin of this phonon energy comes from the infrared absorption study of Stein,¹⁵ who identified a Zn-N local vibration at 553 cm^{-1} (68.6 meV) in polycrystalline ZnSe. We suggest, based on these observations, that the N_I band at 2.54 eV is an intra-center recombination involving a localized excitation coupled with a Zn-N local mode.

We can interpret our N_{II} and N_{III} data in terms of defect energies that have been identified by earlier investigators. If the band gap of ZnSe is taken to be 2.82 eV, then a 170-meV acceptor gives electron-acceptor (e,A) emission at 2.65 eV (i.e., the N_{III} position) and this same 170-meV acceptor gives DAP emission at 2.60 eV (i.e., the N_{II} position) when the deep donor energy of roughly 50 meV is assumed. The energy levels being discussed here may vary by 5 to 10 meV depending on the strength of the pair term in DAP recombination and the uncertainty in the deep donor value. It is interesting to note that a 170-meV acceptor in ZnSe:N has already been suggested by Zhu et al.¹⁶

PL does not provide definitive identifications of the defects in ZnSe epilayers. We thus performed EPR in order to help make defect assignments.² An isotropic signal at $g = 2.0027(3)$ was detected from several layers, as shown in Fig. 4. By assuming a system minimum detection limit of 5×10^{10} spins for a 1 gauss linewidth, we can determine approximate concentrations for the paramagnetic defect centers in the ZnSe layers. The upper trace in Fig. 4 was recorded from an undoped ZnSe epilayer grown under a Zn/Se ratio of 0.63. We conservatively estimate the defect concentration in this film to be about $6 \times 10^{17} \text{ cm}^{-3}$. No EPR signal was detected in a lightly

doped layer grown using a Zn/Se ratio of 0.49, as shown in the second trace in Fig. 4. An increase in nitrogen doping up to $1.5 \times 10^{19} \text{ cm}^{-3}$ produced the signal shown in the third trace of Fig. 4. We estimate the defect concentration in this case to be about $1 \times 10^{17} \text{ cm}^{-3}$. Several additional heavily doped ZnSe:N samples showed similar EPR spectra. The bottom trace in Fig. 4 is from a hydrogen-doped ZnSe epilayer and shows two EPR signals, the one at $g = 2.0027(3)$ and another at $g = 1.9796(3)$. These signals represent concentrations of spins approaching 10^{18} cm^{-3} and mid- 10^{17} cm^{-3} , respectively (note the different signal-to-noise ratio in the lower trace).

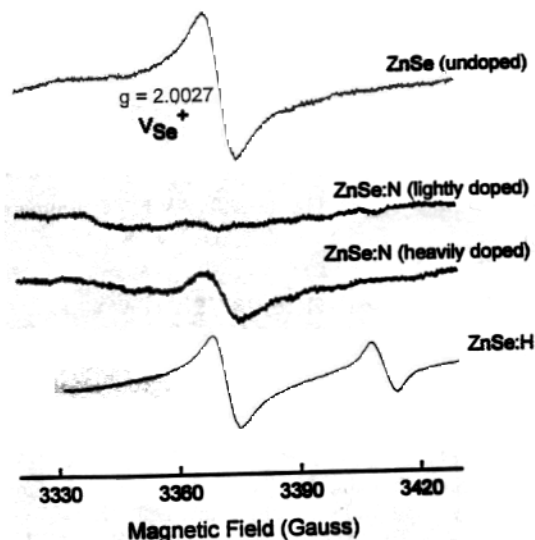


Fig. 4. EPR recorded at 8 K and 9.45 GHz from four ZnSe epilayers.

We assign the EPR signal at $g = 2.0027(3)$ in the ZnSe epilayers grown by MBE to the singly ionized selenium vacancy, V_{Se}^+ , because of the small shift from the free spin g value. The broader linewidth prevents us from determining whether the signal is due to an isolated V_{Se}^+ or a V_{Se}^+ -impurity complex in the various samples. A previous EPR report¹⁷ for electron-irradiated bulk ZnSe assigned the V_{Se}^+ to $g = 2.0085$, which is slightly higher than our observation. We note that our g value is in good agreement with the anion vacancy in ZnS (see Table I). This discrepancy in g -value assignments for the selenium vacancy in ZnSe must be resolved in future studies.

Table I. g values for paramagnetic defects involving the anion vacancy in ZnS and ZnSe.

Material	Defect	g_{\parallel}	g_{\perp}	Reference
ZnS	V_{S}	2.0034	...	18
	$V_{\text{S}}\text{-Cu}_{\text{Zn}}$	2.0061	2.0026	19
	$V_{\text{S}}\text{-Ag}_{\text{Zn}}$	2.0072	2.0024	19
ZnSe	V_{Se}	2.0027(3)	...	this work
	V_{Se}	2.0085(5)	...	17
	$V_{\text{Se}}\text{-X}$	2.0072(2)	2.0013(2)	4

We have identified three PL recombination paths in a heavily nitrogen-doped ZnSe epilayer. The PL bands can be interpreted as intra-center, DAP, and (e,A) recombinations. Our data suggest that spatially separated fluctuations in the band gap are not needed to explain the deep PL data, at least for nitrogen concentrations up to $1.5 \times 10^{19} \text{ cm}^{-3}$. The defect responsible for the intra-center band is not known at this time. Hauksson et al.¹¹ have suggested that the $(V_{\text{Se}}\text{-Zn-N}_{\text{Se}})^+$ complex could be the 50-meV deep donor in ZnSe:N. Our observation of an EPR signal near $g = 2$ suggests that singly ionized selenium vacancies are present in large concentration. The neutral charge state of this complex, $(V_{\text{Se}}^+\text{-Zn-N}_{\text{Se}}^-)^0$, might be the defect responsible for the intra-center recombination. The EPR data indicate this technique will prove useful in studying a variety of undoped and doped ZnSe epilayers.

ACKNOWLEDGEMENTS

This work was supported by the NSF/WV EPSCoR program (NSF Grant OSR-9255224).

REFERENCES

1. K. Prior, *phys. stat. sol. (b)* **187**, 379 (1996).
2. S. D. Setzler, M. Moldovan, Z. Yu, T.H. Myers, N.C. Giles, and L.E. Halliburton, submitted to *Applied Physics Letters*.
3. B.N. Murdin, B.C. Cavenett, C.R. Pidgeon, J. Simpson, I. Hauksson, and K.A. Prior, *Appl. Phys. Lett.* **63**, 2411 (1993).
4. T.A. Kennedy, E.R. Glaser, B.N. Murdin, C.R. Pidgeon, K.A. Prior, and B.C. Cavenett, *Appl. Phys. Lett.* **65**, 1112 (1994).
5. K. Saarinen, T. Laine, K. Skog, J. Makinen, P. Hautajarvi, K. Rakennus, P. Uusimaa, A. Salokatve, and M. Pessa, *Phys. Rev. Lett.* **77**, 3407 (1996).
6. P. Baume, J. Gutowski, D. Wiesmann, R. Heitz, A. Hoffmann, E. Kurtz, D. Hommel, and G. Landwehr, *Appl. Phys. Lett.* **67**, 1914 (1995).
7. C. Kothandaraman, G.F. Neumark, and R.M. Park, *Appl. Phys. Lett.* **67**, 3307 (1995).
8. C. Kothandaraman, I. Kuskovsky, G.F. Neumark, and R.M. Park, *Appl. Phys. Lett.* **69**, 1523 (1996).
9. Z. Yu, S. L. Buczkowski, N.C. Giles, and T.H. Myers, *Appl. Phys. Lett.* **69**, 82 (1996).
10. P.J. Dean, in *Progress in Solid State Chemistry*, edited by J. O. McCaldin and G. Somorjai, (Pergamon Press, New York, 1973), Vol. 8, pp. 1-126.
11. I.S. Hauksson, J. Simpson, S.Y. Wang, K.A. Prior, and B.C. Cavenett, *Appl. Phys. Lett.* **61**, 2208 (1996).
12. Z. Zhu, K. Takebayashi, K. Tanaka, T. Ebisutani, J. Kawamata, and T. Yao, *Appl. Phys. Lett.* **64**, 91 (1994).
13. Z. Zhu, G.D. Brownlie, P.J. Thompson, K.A. Prior, and B.C. Cavenett, *Appl. Phys. Lett.* **67**, 3762 (1995).
14. C. Morhain, E. Tournie, G. Neu, C. Ongaretto, and J.P. Faurie, *Phys. Rev. B* **54**, 4714 (1996).
15. H.J. Stein, *Appl. Phys. Lett.* **64**, 1520 (1994).
16. Z. Zhu, G.D. Brownlie, G. Horsburgh, P.J. Thompson, S.Y. Wang, K.A. Prior, and B.C. Cavenett, *Appl. Phys. Lett.* **67**, 2167 (1995); *J. Cryst. Growth* **159**, 248 (1996).
17. I.A. Gorn, V.N. Martynov, E.S. Volkova, and V.I. Grinev, *Sov. Phys. Semicond.* **24**, 336, (1990).
18. J. Schneider and A. Rauber, *Solid State Commun.* **5**, 779 (1967).
19. J. Dielman, S.H. de Bruin, C.Z. van Doorn, and J.H. Haanstra, *Philips Res. Rep.* **19**, 311 (1964).